# CHANNEL, TREND AND PERIODIC-WISE REPRESENTATION LEARNING FOR MULTIVARIATE LONG-TERM TIME SERIES FORECASTING

Zhangyao Song\*, Nanqing Jiang\*, Miaohong He, Xiaoyu Zhao, Tao Guo™

School of Cyber Science and Engineering, Southeast University, Nanjing, China

## ABSTRACT

Downsampling-based methods for time series forecasting have attracted increasing attention due to their superiority in capturing sequence trends. However, this approaches mainly capture dependencies within subsequences but neglect inter-subsequence and interchannel interactions, which limits forecasting accuracy. To address these limitations, we propose CTPNet, a novel framework that explicitly learns representations from three perspectives: i) inter-channel dependencies, captured by a temporal query-based multi-head attention mechanism; ii) intra-subsequence dependencies, modeled via a Transformer to characterize trend variations; and iii) inter-subsequence dependencies, extracted by reusing the encoder with residual connections to capture global periodic patterns. By jointly integrating these levels, proposed method provides a more holistic representation of temporal dynamics. Extensive experiments demonstrate the superiority of the proposed method.

*Index Terms*— Time series forecasting, downsampling, multiscale dependencies, Transformer.

## 1. INTRODUCTION

Time series forecasting, aims to predict future values based on historical observed time series data, has holds significant applications in fields such as energy management [1], weather forecasting [2], and traffic monitoring [3, 4]. Furthermor, multivariate long-term time series forecasting has received increasing attention, due to it can provide more future information and utilize the dependencies between multiple variables [5–7]. Thanks to advances in deep learning, a variety of methods have been proposed for multivariate long-term time series forecasting, such as Recurrent Neural Network (RNN)-based [8, 9], Convolutional Neural Network (CNN)-based [7, 10–12], Multi-layer Perceptron (MLP)-based [13, 14], and Transformer-based [4, 15, 16] methods. However, the complexity of time series in real-world scenarios limits their capabilities.

In fact, the foundation of accurate long-term time series forecasting lies in the inherent inter-channel dependencies and time dependencies within the data, where time dependencies are further divided into trend and periodic. For inter-channel dependencies, recent studies [5, 6, 15] have employed attention mechanisms, owing to their strong ability to extract multi-level representations. For temporal dependencies, a common strategy in recent works [17–19] is to downsample (see Fig. 1b) the time series into subsequences according to its periodicity, which has demonstrated strong predictive capability. At this stage, each subsequence exhibits the trend variations of the time series, while the relationships across subsequences capture periodic

dependencies. Specifically, [17] employs a weight-shared MLP to extract intra-subsequence dependencies. Since time series often follow fixed periodic patterns (e.g., daily period), each downsampled subsequence tends to exhibit highly similar or consistent trends. However, this approach mainly focuses on dependencies within individual subsequences, while neglecting inter-subsequence dependencies, which results in the loss of valuable temporal information. Moreover, it also overlooks the modeling of inter-channel dependencies [20]. These limitations highlight a fundamental question: how can we design a forecasting framework that effectively learns comprehensive temporal representations across, inter-channel, intra-subsequence, and inter-subsequence dependencies?

In this paper, we address the above limitations by proposing CTPNet (Channel, Trend and Period-wise representation learning **Net**work), a novel framework that performs representation learning on three complementary levels of dependencies: i)  $I_1$  inter-channel dependencies, which capture interactions across variables; ii)  $I_2$  intrasubsequence dependencies, which model local temporal structures within each subsequence; and iii)  $I_3$  inter-subsequence dependencies, which uncover global temporal dynamics across subsequences. Specifically, for inter-channel dependencies, we employ a temporal query-based [5] Multi-Head Attention (MHA, [21]). By using a learnable query matrix Q, the MHA mechanism effectively captures cross-channel dependencies. Secondly, for intra-subsequence dependencies, we adopt a Transformer with linear complexity [22]. The residual connection [23] between the inter-channel dependencies and the original input, followed by linear encoding [13], is used as the Ouery, Key, and Value of the attention mechanism. In this way, the Transformer can effectively capture the complex trend variations (i.e., intra-subsequence dependencies) mapped in the high-dimensional hidden space. Finally, for inter-subsequence dependencies, we use the same network as before. By inputting the transposed encoder output with a residual connection to  $I_2$ , the network can model the inter-subsesquence dependencies.

Using these three perspectives together, CTPNet offers a more holistic representation of time series data, overcoming the limitations of previous methods. Extensive experiments conducted on multiple benchmark datasets demonstrate the superiority of our approach. In a nutshell, our contributions are summarized in three folds:

- Unlike previous methods that only exploit intra-subsequence dependencies within downsampled subsequences, we explicitly model inter-subsequence dependencies.
- We propose CTPNet, a unified framework that simultaneously learns inter-channel, intra-subsequence, and inter-subsequence dependencies for comprehensive representation.
- Through extensive experiments, we establish new state-of-theart performance across multiple benchmarks, demonstrating the robustness and generality of our framework.

<sup>©</sup> Corresponding Author, \* Equivalent Contribution, Email: {zysong, nqjiang, mhhe,xy-zhao, taoguo}@seu.edu.cn, https://github.com/jiangnanqing/CTPNet.git.

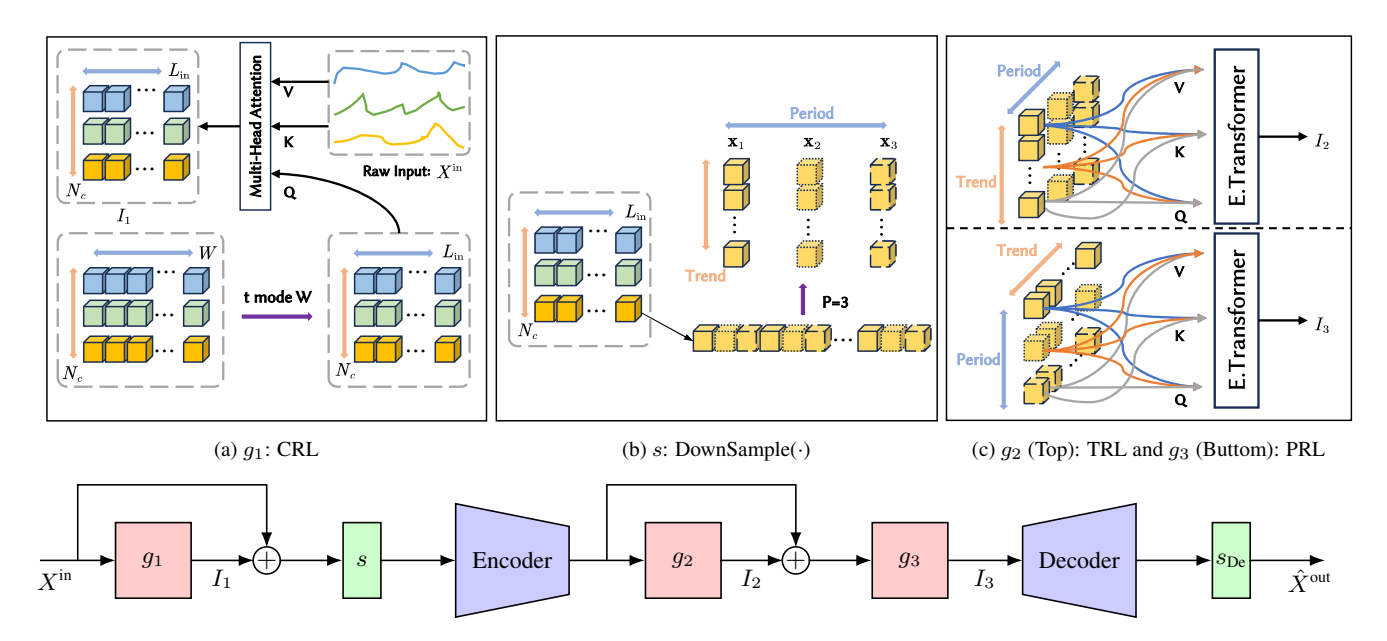


Fig. 1: Overview of CTPNet. Here  $g_1$ ,  $g_2$  and  $g_3$  represent the representation learning networks for inter-channel dependencies, intrasubsequence dependencies, and inter-subsequence dependencies, respectively. s denotes Downsample( $\cdot$ ), and s<sub>De</sub> denotes it's inverse process.

## 2. PRELIMINARIES

## 2.1. Problem Statement

Given a historical series  $X^{\text{in}} = [x_t^{(1:N_c)}, \cdots, x_{t-L_{\text{in}}-1}^{(1:N_c)}] \in \mathbb{R}^{N_c \times L_{\text{in}}}$  of  $L_{\text{in}}$  time steps with  $N_c$  channels (e.g., the number of variables), the goal of time series forecasting (TSF) is to predict the series  $\hat{X}^{\text{out}} = [\hat{x}_{t+L_{\text{out}}}^{(1:N_c)}, \cdots, \hat{x}_{t+1}^{(1:N_c)}] \in \mathbb{R}^{N_c \times L_{\text{out}}}$  of the next  $L_{\text{out}}$  time steps based on  $X^{\text{in}}$ , and to minimize the difference between  $\hat{X}^{\text{out}}$  and the target  $X^{\text{target}}$ . It can be formulated as

$$[\hat{x}_{t+L_{\text{out}}}^{(1:N_c)},\cdots,\hat{x}_{t+1}^{(1:N_c)}] = f\left([x_t^{(1:N_c)},\cdots,x_{t-L_{\text{in}}-1}^{(1:N_c)}]\right), \quad (1)$$

where f represents a trainable neural network.

## 2.2. Time Series Downsampling

Given a time series  $X = [x_t^{(n)}, \cdots, x_{t-L_{\text{in}}-1}^{(n)}]$  with periodicity P, the operation of downsampling [17] decomposes the sequence into P downsampled subsequences of length  $N_{\text{pin}} = \lfloor \frac{L_{\text{in}}}{P} \rfloor$ . As shown in Fig. 1b, it can be formulated as

$$[\mathbf{x}_1, \cdots, \mathbf{x}_P] = \text{DownSample}(X),$$
 (2)

where  $\mathbf{x}_p = [x_{t+p-1+0\times P}, \cdots, x_{t+p-1+(N_{\text{pin}}-1)\times P}] \in \mathbb{R}^{N_{\text{pin}}}$  denotes the p-th subsequence. Meanwhile, we denote the inverse process of DownSample(·) as De-DownSample(·).

## 3. METHOD: CTPNET

#### 3.1. Structure Overview

As illustrated in Fig. 1, the proposed CTPNet consists of seven key components: ① Channel-wise Representation Learning (CRL) captures inter-channel dependencies; ② Downsample( $\cdot$ ) downsamples the residual connection of  $I_1$  and the original input to generate multiple subsequences; ③ Encoder maps each subsequence of

length  $N_{\rm pin}$  into a D-dimensional representation; ( Trend-wise Representation Learning (TRL) captures intra-subsequence dependencies; ( Periodic-wise Representation Learning (PRL) captures intersubsequence dependencies; ( Decoder converts the subsequence length from D back to  $N_{\rm pout}$ , enabling the next operation to yield a prediction horizon of length  $L_{\rm out}$ ; ( De-Downsample(·) recombines the multiple subsequences into a single sequence.

## 3.2. Channel-wise Representation Learning (CRL)

Here, we adopt the Temporal Query (TQ, [5]) technique to model inter-channel dependencies  $I_1$ . As shown in Fig. 1a, this method introduces periodically shifted learnable vectors as queries to mitigate the impact of noise and missing values on local correlations, while the raw input sequence serves as keys and values to preserve instance-level information. In this way, the attention mechanism integrates both global priors and local features. Specifically, given a period length W, we define the learnable parameters  $\theta^{TQ} \in \mathbb{R}^{N_c \times W}$ , and at time step t, a segment of length  $L_{\rm in}$  is selected as the query

$$Q = \theta_{t, L_{\text{in}}}^{TQ} \in \mathbb{R}^{N_c \times L_{\text{in}}}, \tag{3}$$

where the index is determined by  $t \mod W$ , enabling periodic parameter reuse. The input sequence  $X_t$  is linearly projected to obtain keys and values

$$K_1 = X_t W^{K_1}, \quad V_1 = X_t W^{V_1},$$
 (4)

and the attention is computed as

$$\operatorname{Head}_{h} = \operatorname{Softmax}\left(\frac{Q_{h}K_{h}^{\top}}{\sqrt{L_{\operatorname{in}}}}\right)V_{h}. \tag{5}$$

MHA mechanism concatenates the outputs

$$I_1 = \text{MHA}(Q, K_1, V_1) = \text{Concat}(\text{head}_1, \dots, \text{head}_H) W^O,$$
 (6)

where  $W^O$  is a learnable projection matrix.

 $\label{eq:table_loss} \textbf{Table 1} \\ \textbf{MULTIVARIATE TIME SERIES FORECASTING RESULTS}.$ 

MODEL		CTPNET (OURS)		TQNET [5] (2025)		TWINS* [24] (2025)		LEDDAM [20] (2024)		ITRANS* [15] (2024)		PATCHTST [16] (2023)		CROSS* [6] (2023)		FED* [1] (2022)	
M	IETRIC	MSE	MAE	MSE	MAE	MSE	MAE	MSE	MAE	MSE	MAE	MSE	MAE	MSE	MAE	MSE	MAE
	96	0.363	0.388	0.371	0.393	0.385	0.401	0.377	0.394	0.386	0.405	0.414	0.419	0.423	0.448	0.376	0.419
Тн	192	0.414	0.416	0.428	0.426	0.439	0.431	0.424	0.422	0.441	0.436	0.460	0.445	0.471	0.474	0.420	0.448
ET	336	0.453	0.435	0.476	0.446	0.480	0.452	0.459	0.442	0.487	0.458	0.501	0.466	0.570	0.546	0.459	0.465
	720	0.451	0.451	0.487	0.470	0.480	0.474	0.463	0.459	0.503	0.491	0.500	0.488	0.653	0.621	0.506	0.507
Тн2	96	0.287	0.336	0.295	0.343	0.292	0.345	0.292	0.343	0.297	0.349	0.302	0.348	0.745	0.584	0.358	0.397
Ę	192	0.356	0.381	$\frac{0.367}{0.417}$	0.393	0.375	0.395	0.367	$\frac{0.389}{0.424}$	0.380	0.400	0.388	0.400	0.877	0.656	0.429	0.439
EI	336	0.412	<b>0.422</b> 0.433	0.417	0.427 $0.446$	0.417	0.429 <b>0.430</b>	0.412 0.419	$\frac{0.424}{0.438}$	$0.428 \\ 0.427$	0.432	0.426 0.431	0.433 0.446	1.043	0.731	0.496 $0.763$	0.487 $0.474$
	720 96	0.410	0.433	0.433	0.446	0.406	0.364	0.419	0.438	0.427	0.445	0.431	0.446	$\frac{0.463}{0.404}$	0.426	0.763	0.474
$\Xi$	192	0.310 $0.359$	$0.340 \\ 0.376$	$\frac{0.311}{0.356}$	$\frac{0.333}{0.378}$	0.323	0.304	0.319	0.339	0.334	0.308	0.329	0.385	0.404	0.420	0.379	0.419
TTM	336	$\frac{0.339}{0.387}$	0.376	0.390	$\frac{0.378}{0.401}$	0.406	0.330	0.394	0.363	0.426	0.420	0.399	0.383	0.430	0.431	0.426	0.459
団	720	0.449	0.434	$\frac{0.350}{0.452}$	$\frac{0.401}{0.440}$	0.467	0.448	0.460	0.442	0.491	0.459	0.454	0.439	0.666	0.589	0.543	0.490
7	96	0.174	0.251	0.173	0.256	0.173	0.256	0.176	0.257	0.180	0.264	0.175	0.259	0.287	0.366	0.203	0.287
Z	192	0.238	0.294	0.238	$\frac{0.228}{0.298}$	0.239	$\frac{0.300}{0.300}$	0.243	0.303	0.250	0.309	0.241	0.302	0.414	0.492	0.269	0.328
ЕТТМ2	336	0.299	0.333	0.301	0.340	0.298	0.339	0.303	0.341	0.311	0.348	0.305	0.343	0.597	0.542	0.325	0.366
団	720	0.399	0.392	0.397	0.396	0.397	0.397	0.400	0.398	0.412	0.407	0.402	0.400	1.730	1.042	0.421	0.415
	96	0.134	0.224	0.134	0.229	0.139	0.233	0.141	0.235	0.148	0.240	0.181	0.270	0.219	0.314	0.193	0.308
CL	192	0.151	0.240	0.154	0.247	0.158	0.252	0.159	0.252	0.162	0.253	0.188	0.274	0.231	0.322	0.201	0.315
$reve{\mathbf{m}}$	336	0.166	0.256	0.169	0.264	0.172	0.267	0.173	0.268	0.178	0.269	0.204	0.293	0.246	0.337	0.214	0.329
	720	0.200	0.286	0.201	0.294	0.200	0.293	0.201	0.295	0.225	0.317	0.246	0.324	0.280	0.363	0.246	0.355
R	96	0.168	0.223	0.173	0.233	0.193	0.224	0.197	0.241	0.203	0.237	0.234	0.286	0.310	0.331	0.242	0.342
LA	192	0.184	0.238	0.199	0.257	0.223	0.250	0.231	0.264	0.233	0.261	0.267	0.310	0.734	0.725	0.285	0.380
So	336	0.200	0.254	$\frac{0.211}{0.200}$	$\frac{0.263}{0.270}$	0.246	0.268	0.241	0.268	0.248	0.273	0.290	0.315	0.750	0.735	0.282	0.376
7.)	720	0.204	0.247	0.209	0.270	0.245	0.272	0.250	0.281	0.249	0.275	0.289	0.317	0.769	0.765	0.357	0.427
HC	96 192	0.398	$0.251 \\ 0.261$	0.413 0.432	0.261 0.271	$0.382 \\ 0.392$	0.260 0.267	0.426 0.458	$0.276 \\ 0.289$	$\frac{0.395}{0.417}$	0.268 0.276	0.462 0.466	0.290 0.290	0.522 0.530	0.290	0.587 0.604	0.366 0.373
RAFFI	336	0.419	$0.201 \\ 0.270$	0.452	0.277	0.392	$\frac{0.267}{0.276}$	0.436	0.289	$\frac{0.417}{0.433}$	0.270	0.482	0.290	0.558	0.293	0.621	0.373
5	720	0.470	0.270	0.486	0.277	0.410	$\frac{0.270}{0.292}$	0.498	0.313	$\frac{0.433}{0.467}$	0.302	0.432	0.320	0.589	0.303	0.626	0.383
<u> </u>	96	0.156	0.196	0.157	0.200	0.161	0.201	0.156	0.202	0.174	0.214	0.177	0.210	0.158	0.230	0.020	0.296
EATHER	192	0.130	0.170	0.137	$\frac{0.200}{0.245}$	0.211	0.248	0.207	0.250	0.221	0.254	0.225	0.250	0.136	0.277	0.276	0.336
Ė	336	0.262	0.285	$\frac{0.262}{0.262}$	$\frac{0.287}{0.287}$	0.266	0.291	0.262	0.291	0.278	0.296	0.278	0.290	$\frac{0.233}{0.272}$	0.335	0.339	0.380
	720	0.343	0.340	0.344	0.342	0.347	0.343	0.343	0.343	0.358	0.349	0.354	0.340	0.398	0.418	0.403	0.428
₹ <sub>IST</sub>	Count	5	4	(	5	1	0	۷	1	(	)		1	(	)	(	)

The look-back length  $L_{\rm in}$  is fixed at 96, and "\*" denotes "former".

**Remark 1.** It is worth noting that the period W here differs from the one used in downsampling. For downsampling, a large period would result in overly sparse sequences and loss of temporal information, thus the smallest inherent period (e.g., daily period of 24) is usually adopted. In contrast, in the TQ mechanism, the query Q is designed to capture long-range periodic variations, and therefore a longer period (e.g., weekly period of 168) is preferred. Both types of periods can be determined via the autocorrelation function (ACF, [25]).

We perform a residual connection between  $I_1$  and the original input  $X^{\mathrm{in}}$ , formulated as

$$X^{\text{in}'} \in \mathbb{R}^{N_c \times L_{\text{in}}} = X^{\text{in}} + I_1, \tag{7}$$

to enhance training stability. After that, downsampling (as introduced in Sec. 2.2) is applied

$$X_{ds}^{in'} \in \mathbb{R}^{N_c \times P \times N_{pin}} = \text{DownSample}(X^{in'}),$$
 (8)

and the resulting P subsequences are fed into the following networks.

## 3.3. Trend-wise Representation Learning (TRL)

The downsampled subsequences are processed by a linear (a Full-Connect network) encoder, which maps the temporal dimension after downsampling into a *D*-dimensional hidden space

$$Z \in \mathbb{R}^{N_c \times P \times D} = \text{Encoder}(X_{ds}^{\text{in}'}).$$
 (9)

Prior studies [13, 14, 17] have shown that this setup allows neural networks to extract richer features in the higher-dimensional

hidden space while alleviating the sparsity issue caused by wide intervals in downsampling. Afterward, the TRL network captures intra-subsequence temporal dependencies  $I_2$  within the hidden space, as illustrated in Fig. 1c Top (where "E." denotes the "Efficient"). Specifically, we adopt an efficient attention [22] to extract  $I_2$ , defined

$$E_2 = \text{Attention}(Q_2, K_2, V_2) = \rho(Q_2) \left( \rho(K_2^\top) \cdot V_2 \right),$$
 (10)

where  $\rho(\cdot)$  denotes  $\frac{\cdot}{\sqrt{\dim(\cdot)}}$  and

$$Q_2 = ZW^{Q_2}, \quad K_2 = ZW^{K_2}, \quad V_2 = ZW^{V_2},$$
 (11)

with  $W^{Q_2},W^{K_2},W^{V_2}$  being learnable weight matrices.  $E_2$  will be input into a MHA, following an operation similar to that in Eq. (12), to obtain  $E_2^{(\mathrm{mha})}$ . Then,  $E_2^{(\mathrm{mha})}$  is input into the Transformer network

$$I'_{2} = \operatorname{LayerNorm}(Z + E_{2}^{(\operatorname{mha})}),$$

$$I''_{2} = \operatorname{Linear}\left(\operatorname{GeLU}\left(\operatorname{Linear}(I'_{2})\right)\right),$$

$$I_{2} = \operatorname{LayerNorm}\left(I'_{2} + I''_{2}\right),$$
(12)

where Linear (GeLU (Linear( $\cdot$ ))) represents a multi-layer feedforward network (Linear is the Full-connected network, and GeLU is a activation function), and LayerNorm( $\cdot$ ) denotes layer normalization.

## 3.4. Periodic-wise Representation Learning (PRL)

The network used to extract  $I_3$  has exactly the same structure as the network used to extract  $I_2$ . When the feature dimensions input to the network differ, it is capable of capturing dependencies of different

Table 2 Ablation Results of CTPNet.

ABLA	ΓΙΟΝ	FULL	$I_1$	$I_2$	$I_3$	$I_1, I_2$	$I_1, I_3$	$I_{2}, I_{3}$
ЕТТн2	MSE MAE	$0.366 \\ 0.393$	$\frac{0.369}{0.395}$		0.384 0.402			0.385 0.408
ЕТТм2	MSE MAE	$0.278 \\ 0.318$	$\frac{0.279}{0.320}$	0.280	0.281		0.285 0.324	
ECL	MSE MAE	$0.163 \\ 0.252$	$0.190 \\ 0.270$	$\frac{0.170}{0.258}$	$0.176 \\ 0.265$		0.207 0.284	0.190
SOLAR	MSE MAE	$0.189 \\ 0.241$	$0.221 \\ 0.260$	$\frac{0.193}{0.243}$	$0.197 \\ 0.254$		$0.264 \\ 0.310$	$0.268 \\ 0.350$
TRAFFIC	MSE MAE	$0.431 \\ 0.268$	0.454 $0.278$		$\frac{0.448}{0.292}$		$0.510 \\ 0.321$	$0.530 \\ 0.334$

The results are averaged over four prediction horizons.

dimensions. To extract  $I_3$ , a transpose is first performed to move the subsequence dimension to the last axis, as illustrated in Fig. 1c bottom. At the same time, the operations in Equations (10) to (12) are carried out, which we denote concisely as

$$I_3 = g_3 \left( (Z + I_2)^\top \right)^\top, \tag{13}$$

At this point, the network can effectively extract  $I_3$ . Subsequently, the linear decoder projects the learned representations onto the target prediction time domain  $\hat{X}_{\mathrm{ds}}^{\mathrm{out}} = \mathrm{Decoder}\left(I_3\right)$ . It then combines them through inverse downsampling

$$\hat{X}^{\text{out}} = \text{De-DownSample}\left(\hat{X}^{\text{out}}_{\text{ds}}\right),$$
 (14)

to form a predicted tensor of length  $L_{\text{out}}$ , where  $\hat{X}^{\text{out}} \in \mathbb{R}^{N_{\text{c}} \times L_{\text{out}}}$  denotes the predicted results.

#### 4. EXPERIMENT

The performance of the proposed CTPNet is evaluated on eight widely used benchmark datasets, including ETT (ETTh1, ETTh2, ETTm1, ETTm2), Weather, Electricity (ECL), Traffic, and Solar. The data preprocessing procedure is consistent with prior works [5], including the instance normalization strategy. All experiments were implemented using the PyTorch framework and executed on an NVIDIA RTX 4090 GPU equipped with 24 GB of memory. The training objective used a L1 loss is optimized using the Adam optimizer [26].

## 4.1. Long-term Forecasting

**Setups.** We conducted performance evaluation of the CTPNet against seven mainstream methods, including TQNet [5], Twinsformer [27], Leddam [20], iTransformer [15], PatchTST [16], Crossformer [6], and FEDformer [1]. For long-term forecasting, following prior works [4, 5, 15, 28], we set the prediction horizons to  $L_{\rm out} \in \{96, 192, 336, 720\}$ , while fixing the look-back window length to  $L_{\rm in} = 96$ . For performance evaluation, Mean Squared Error (MSE) and Mean Absolute Error (MAE) were employed as evaluation metrics. The best results are highlighted in **bold**, while the second-best results are underlined.

**Result Analysis.** As shown in Tab. 1, we present a comparison of the prediction performance between CTPNet and baseline models across eight real-world datasets. Specifically, compared with TQNet [5] and Crossformer [6], CTPNet reduces MSE/MAE by 2.22%/2.45%, 19.37%/19.29% respectively, in terms of the average across all cases. On the datasets with pronounced periodic variations (ETTh1, ETTh2, and Solar), CTPNet consistently outperforms the runner-up TQNet, reducing MSE/MAE by 4.76%/2.53%, 3.17%/2.24%, and 4.55%/5.86%, respectively. Overall, out of 64 evaluation metrics, CTPNet ranks within the top two in 58 cases, including 54 first-place results.

Table 3
PERFORMANCE OF DIFFERENT INTERVAL ON ETTH1.

INTERVAL		2	4			3	1	6	24	
Horizon	MSE	MAE	MSE	MAE	MSE	MAE	MSE	MAE	MSE	MAE
96 192		0.392 0.420								
336 720		0.438 0.458				$0.462 \\ 0.509$				

#### 4.2. Ablation Studies

#### 4.2.1. Ablation on $I_1$ , $I_2$ , and $I_3$

As shown in Tab. 2, when removing  $I_1$ ,  $I_2$ , and  $I_3$  respectively, we find that in the ETTh2 and ETTm2 datasets, the model incurs the highest accuracy loss when  $I_3$  is removed. This verifies that the interdependencies between cycles are relatively strong in these two datasets. This indicates that in datasets like ETT, which exhibit clear periodic variations, the dependencies within cycles (inter-subsequence dependencies) are relatively prominent. Moreover, when  $I_1$  is removed, the decline in prediction performance is the least noticeable. This is because ETT has only 7 channels, and the dependencies between channels are relatively weak. In contrast, in the ECL ( $N_c = 321$ ), Solar ( $N_c = 137$ ), and Traffic ( $N_c = 862$ ) datasets with a large number of channels, the accuracy loss when removing  $I_1$  is significantly higher than that when removing the other two dependencies, which further verifies the effectiveness of the  $I_1$  dependencies.

Furthermore, it can be observed from the table that when any two of  $I_1$ ,  $I_2$ , and  $I_3$  are removed simultaneously, the model's accuracy decreases compared to removing only one. In particular, removing  $I_2$  and  $I_3$  leads to the greatest accuracy reduction, whether on datasets with fewer channels like ETTh2 and ETTm2 or on datasets with more channels like ECL, Solar, and Traffic. This indicates that merely modeling inter-channel dependencies is far from sufficient, thereby verifying the necessity of intra-subsequence modeling and inter-subsequence modeling in this paper. Across all scenarios, the ablated models consistently underperform compared to the full model.

#### 4.2.2. Impact of Downsampling Interval

This section primarily discusses the impact of setting incorrect down-sampling intervals on model performance during the downsampling process. We validate this through ablation experiments by setting different downsampling intervals (2, 4, 8, 16, 24) on the ETTh1 dataset. Notably, the minimum period calculated via ACF is 24 (daily period). As shown in Tab. 3, when the downsampling interval is set to 24, the model's performance outperforms other downsampling interval settings. This indicates that selecting a downsampling interval that matches the data period helps better capture periodic patterns in the time series, thereby improving prediction performance. Additionally, when the downsampling interval is set to 2 or 4, the model also performs well, likely because smaller downsampling intervals can capture the trends in the time series at a finer granularity.

## 5. CONCLUSION

In this paper, we addressed the challenge of capturing complex dependencies in time series forecasting. Unlike existing approaches that mainly focus on temporal dependencies within downsampled subsequences, we highlighted the critical role of inter-subsequence dependencies. To this end, we proposed CTPNet, a novel framework that jointly models inter-channel, intra-subsequence, and intersubsequence dependencies, enabling more comprehensive representation learning. Extensive experiments across multiple real-world datasets validated the effectiveness of our method.

## References

- [1] T. Zhou, Z. Ma, Q. Wen, et al., "FEDFormer: Frequency enhanced decomposed transformer for long-term series forecasting," in *International Conference on Machine Learning*, 2022.
- [2] R. Ilbert, A. Odonnat, V. Feofanov, et al., "Samformer: Unlocking the potential of transformers in time series forecasting with sharpness-aware minimization and channel-wise attention," in *Proceedings of the 41st International Conference on Machine Learning*, vol. 235, PMLR, 2024. [Online]. Available: https://proceedings.mlr.press/v235/ilbert24a.html
- [3] G. Woo, C. Liu, D. Sahoo, et al., "ETSformer: Exponential smoothing transformers for time-series forecasting," *arXiv* preprint arXiv:2202.01381, 2022.
- [4] H. Zhou, S. Zhang, J. Peng, et al., "Informer: Beyond efficient transformer for long sequence time-series forecasting," in Proceedings of the AAAI Conference on Artificial Intelligence, 2021
- [5] S. Lin, H. Chen, H. Wu, et al., "Temporal query network for efficient multivariate time series forecasting," in *Forty-second International Conference on Machine Learning*, 2025.
- [6] Y. Zhang and J. Yan, "Crossformer: Transformer utilizing cross-dimension dependency for multivariate time series forecasting," in *International Conference on Learning Represen*tations, 2023.
- [7] E. Zhang, W. Yuan, and X. Liu, "Channelmixer: A hybrid contransformer framework for enhanced multivariate long-term time series forecasting," in *IEEE International Conference on Acoustics, Speech and Signal Processing*, 2025. DOI: 10.1109/ICASSP49660.2025.10887797
- [8] S. Lin, W. Lin, W. Wu, et al., Segrnn: Segment recurrent neural network for long-term time series forecasting, 2023. arXiv: 2308.11200 [cs.LG]. [Online]. Available: https:// arxiv.org/abs/2308.11200
- [9] X. Zhang, C. Zhong, J. Zhang, et al., "Robust recurrent neural networks for time series forecasting," *Neurocomputing*, 2023.
- [10] L. donghao and wang xue, "ModernTCN: A modern pure convolution structure for general time series analysis," in *The Twelfth International Conference on Learning Representations*, 2024. [Online]. Available: https://openreview.net/forum?id=vpJMJerXHU
- [11] S. Bai, J. Z. Kolter, and V. Koltun, "An empirical evaluation of generic convolutional and recurrent networks for sequence modeling," arXiv preprint arXiv:1803.01271, 2018.
- [12] M. Liu, A. Zeng, M. Chen, et al., "SCINet: Time series modeling and forecasting with sample convolution and interaction," *Advances in Neural Information Processing Systems*, 2022.
- [13] A. Zeng, M. Chen, L. Zhang, et al., "Are transformers effective for time series forecasting?" In *Proceedings of the AAAI Conference on Artificial Intelligence*, 2023.
- [14] S. Lin, W. Lin, X. Hu, et al., "Cyclenet: Enhancing time series forecasting through modeling periodic patterns," *Advances in Neural Information Processing Systems*, vol. 37, pp. 106 315– 106 345, 2024.

- [15] Y. Liu, T. Hu, H. Zhang, et al., "iTransformer: Inverted transformers are effective for time series forecasting," in *The Twelfth International Conference on Learning Representations*, 2024.
- [16] Y. Nie, N. H. Nguyen, P. Sinthong, et al., "A time series is worth 64 words: Long-term forecasting with transformers," in *International Conference on Learning Representations*, 2023.
- [17] S. Lin, W. Lin, W. Wu, et al., "SparseTSF: Modeling long-term time series forecasting with 1k parameters," in Forty-first International Conference on Machine Learning, 2024.
- [18] H. Wu, T. Hu, Y. Liu, et al., "TimesNet: Temporal 2d-variation modeling for general time series analysis," in *International Conference on Learning Representations*, 2023.
- [19] S. Wang, J. LI, X. Shi, et al., "Timemixer++: A general time series pattern machine for universal predictive analysis," in *The Thirteenth International Conference on Learning Representations*, 2025. [Online]. Available: https://openreview.net/forum?id=1CLzLXSFNn
- [20] G. Yu, J. Zou, X. Hu, et al., "Revitalizing multivariate time series forecasting: Learnable decomposition with Inter-Series dependencies and intra-series variations modeling," in *Forty*first International Conference on Machine Learning, 2024.
- [21] A. Vaswani, N. Shazeer, N. Parmar, et al., "Attention Is All You Need," in Advances in Neural Information Processing Systems, 2017.
- [22] Z. Shen, M. Zhang, H. Zhao, et al., "Efficient attention: Attention with linear complexities," CoRR, vol. abs/1812.01243, 2018. [Online]. Available: http://arxiv.org/abs/1812.01243
- [23] K. He, X. Zhang, S. Ren, et al., "Deep residual learning for image recognition," in *Proceedings of the IEEE conference on* computer vision and pattern recognition, 2016, pp. 770–778.
- [24] A. Stitsyuk and J. Choi, "Xpatch: Dual-stream time series forecasting with exponential seasonal-trend decomposition," in *Proceedings of the AAAI Conference on Artificial Intelli*gence, vol. 39, 2025, pp. 20601–20609.
- [25] H. Madsen, Time series analysis. CRC Press, 2007.
- [26] D. P. Kingma and J. Ba, "Adam: A method for stochastic optimization," CoRR, vol. abs/1412.6980, 2014. [Online]. Available: https://api.semanticscholar.org/ CorpusID:6628106
- [27] Y. Zhou, Y. Ye, P. Zhang, et al., Twinsformer: Revisiting inherent dependencies via two interactive components for time series forecasting, 2025. [Online]. Available: https: //openreview.net/forum?id=BSsyY29bc1
- [28] H. Wu, J. Xu, J. Wang, et al., "Autoformer: Decomposition transformers with auto-correlation for long-term series forecasting," Advances in Neural Information Processing Systems, 2021.